[redacted]

COSMIC RAY GROUP

Department of Physics

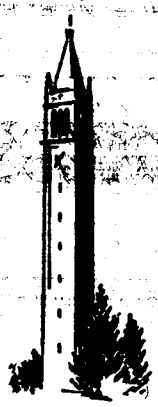

UNIVERSITY OF CALIFORNIA

BERKELEY

DAYTIME OBSERVATIONS OF ENERGETIC AURORAL ZONE ELECTRONS

M. Lampton
Department of Physics
University of California, Berkeley

April, 1967

ABSTRACT

Daytime electron precipitation has been observed from on board Nike Apache sounding rockets launched from Fort Churchill, Manitoba, Canada. Energy spectra and pitch angle distributions are presented. Rapid time variations are seen at energies greater than 60 keV, and travel time arguments indicate that the precipitation cause acts within a few R_e of the earth.

INTRODUCTION

The existence of daytime auroral-zone electron precipitation has been well established. Results of high latitude satellite observations and stratosphere balloon-borne X-ray counter surveys show that substantial fluxes of electrons with energy above 40 kilovolts reach the auroral zone atmosphere, particularly during the main and recovery phases of magnetic storms (O'Brien, 1964; Brown, 1966). In particular, the negligibly small motion of balloon payloads during the time scale of many kinds of events has permitted study and classification of the time structure of these events. Results of such studies have been to identify long period variations, with scale times exceeding one minute, with the action of hydromagnetic waves on the magnetospheric electron population (Anderson et al., 1966; Barcus and Rosenberg, 1965; Barcus and Christiansen, 1965) while large amplitude shorter period flux variations have been ascribed to plasma instabilities (Coppi, 1965) or to dynamics of trapped electron motion (Anderson and Milton, 1964; see also Chamberlain, 1963).

In order to more closely examine the details of daytime electron precipitation, Nike Apache sounding rocket payloads were instrumented for performance direct measurements of the absolute intensity, energy spectrum, and pitch angle distribution of these electron fluxes. The amount of data collection time (several hundred seconds) and the sufficiently slow rate of travel across magnetic field lines (100 meters per second) permit identification of short period time structure in the precipitating flux.

INSTRUMENTATION

The primary apparatus on each payload was a pair of plastic phosphor scintillation counters, orthogonally oriented to view electron intensities in directions parallel and perpendicular to the rocket spin axis. Each was

equipped with a three-channel differential pulse height analyzer, intended to provide a rough energy spectrum measurement with windows of 60-90 keV, 90-150 keV, and 150-300 keV. An aluminum absorber of thickness 3 mg/cm^2 covered each phosphor and stopped sunlight and protons having energy less than 800 keV. Passive collimation defined an effective area of 0.18 cm^2 with a 14° half angle.

In addition, a pair of Channeltrons were integrated into each payload, having collimators and selector magnets giving maximum geometry factors at 7 keV and 13 keV, with energy resolutions of $\pm$ 30% at half-maximum. These detectors had a 2° field of view, parallel to the rocket axis. Counting rates seen in all information channels were logarithmically compressed over a five decade range before analog transmission to the ground receiving station.

Spin stabilization of the payloads was employed. Due to the asymmetric ejection of the payload nose cones, during most of each flight the rocket spin axis moved slowly around a cone of approximately 15° half angle. This motion allowed the axially oriented detectors to view a range of charged particle pitch angles centered between 5° and 35°. Radially oriented detectors viewed corresponding intervals of 85-95° and 55-125°. The rocket aspect was monitored by two fluxgate magnetometers.

GEOPHYSICAL CONDITIONS

A number of balloon launches were made from Ft. Churchill during September, 1965, with the objective of identifying times of daytime electron precipitation by means of measuring atmospheric X-ray bremsstrahlung. During the magnetic storm which began on 15 September, auroral zone X-rays were observed intermittently for five days. Of particular interest here is the highly time structured X-ray flux seen on 17 September during considerable worldwide

geomagnetic activity (three hour average $K_p = 4-$). At this time one rocket was successfully launched. During a magnetically quiet ($K_p = 1+$) post-recovery period further strong but unstructured X-ray activity was measured and a second successful rocket flight was made. The data reported here were taken during the first of these flights.

RESULTS OF 17 SEPTEMBER FLIGHT

Electron fluxes seen on 17 September 1965 are presented in Figure 1 as a function of time, along with the altitude and the aspect angle between the rocket axis and the local geomagnetic field. It is seen that the lower energy particles undergo a slow decrease in flux throughout the flight, seen here modulated by the payload's varying aspect, while a number of prominent enhancements of electrons above 60 keV occur. It is convenient to separate this flight into the first portion, 140-240 sec, during which the energetic electrons are highly anisotropic and appear to have only brief intervals of low-level impulsive precipitation, and the second portion (270-330 sec) in which much larger fluxes and more persistent time structure were seen.

A comparison of counting rates of the several energy channels enables us to construct differential energy spectra for the two portions of the flight. Figure 2 illustrates these distributions obtained for the axially oriented electron counters; dashed portions of each curve are energy intervals inaccessible to these detectors and represent interpolations. The observed e-folding energies, which ranged from 6 to 30 keV, represent softer spectra than other workers have seen at lower latitude or higher energy (Blake et al., 1966; Mozer, 1965). However, we find good agreement with inferences drawn from several balloon observations (Barcus and Rosenberg, 1966) and rocket measurements (McDiarmid and Budzinski, 1964).

geomagnetic activity (three hour average $K_p = 4-$). At this time one rocket was successfully launched. During a magnetically quiet ($K_p = 1+$) post-recovery period further strong but unstructured X-ray activity was measured and a second successful rocket flight was made. The data reported here were taken during the first of these flights.

RESULTS OF 17 SEPTEMBER FLIGHT

Electron fluxes seen on 17 September 1965 are presented in Figure 1 as a function of time, along with the altitude and the aspect angle between the rocket axis and the local geomagnetic field. It is seen that the lower energy particles undergo a slow decrease in flux throughout the flight, seen here modulated by the payload's varying aspect, while a number of prominent enhancements of electrons above 60 keV occur. It is convenient to separate this flight into the first portion, 140-240 sec, during which the energetic electrons are highly anisotropic and appear to have only brief intervals of low-level impulsive precipitation, and the second portion (270-330 sec) in which much larger fluxes and more persistent time structure were seen.

A comparison of counting rates of the several energy channels enables us to construct differential energy spectra for the two portions of the flight. Figure 2 illustrates these distributions obtained for the axially oriented electron counters; dashed portions of each curve are energy intervals inaccessible to these detectors and represent interpolations. The observed e-folding energies, which ranged from 6 to 30 keV, represent softer spectra than other workers have seen at lower latitude or higher energy (Blake et al., 1966; Mozer, 1965). However, we find good agreement with inferences drawn from several balloon observations (Barcus and Rosenberg, 1966) and rocket measurements (McDiarmid and Budzinski, 1964).

The combination of vehicle spin and precession during flight allows a range of pitch angles to be viewed by the pair of scintillation counters. By calculating flux averaged over those time intervals corresponding to a given small range of pitch angle, the angular distribution of energetic electrons is obtained. This distribution is shown in Figure 3, where no corrections have been made for the angular sensitivity of the detectors. It is clear that the electron intensity remains strongly peaked near 90°, except very late in the flight when atmospheric scattering is appreciable. It is further evident, both from this and from Figure 1, that enhanced precipitation is fractionally greater at smaller pitch angles, i.e. well inside the loss cone. Such enhancements, then, are associated with a more nearly isotropic pitch angle distribution over $0 - 90^{\circ}$, in agreement with McDiarmid (McDiarmid and Budzinski, 1964). Between 100° and 125°, the intensity is at most 10% of its magnitude at 60°, and consequently this albedo can probably be explained by atmospheric scattering.

Both portions of this flight have revealed rapid time structure in the electron flux at energies greater than 60 keV. During the more intense second portion of the flight we observe that the salient characteristics of this structure are the 0.2 sec duration of a typical pulse, the approximately 20 keV e-folding energy of the electron spectrum at a peak, and the close time association of the pulse seen in the various energy and pitch-angle channels. A few seconds of this activity can be seen in Figure 4. This characteristic time structure permits identification of these electrons as responsible for the production of X-ray microbursts. The intensity and energy spectrum of the parent electrons as deduced from prior X-ray measurements also support such an interpretation (Hudson et al., 1965). No detailed correspondence between rocket and balloon count rates were observed on this flight, presumably due to the

considerable horizontal separation of these vehicles. It is worthwhile to note the large, rather steadier electron intensity seen near 90° pitch angle, which may be responsible for the enhanced X-ray background customarily associated with balloon microburst observations. Microburst electrons are seen at 90°, and in roughly the same number as at 0°; the fractional change at 90° is less than at 0° due to the additional steady mirroring electrons.

Another characteristic of this intense precipitation is the frequent appearance or disappearance of the electron flux on a time scale of 10-30 milliseconds. Such events are illustrated in Figure 4, in which ten-millisecond count rate averages are plotted. A gap in one microburst, lasting approximately 0.03 sec, is seen; also shown is another microburst having rise and fall times of only a few milliseconds.

Large amplitude fast variations in the electron flux permit a sensitive test for the degree of association of the modulating phenomenon between the various energy channels. One quantitative measure of possibly delay in arrival of lower energy electrons is provided by a cross-correlation analysis. Here, fifteen seconds of count-rate data from the axial scintillation counter were used; the result is shown in Figure 5. It is seen that during this portion of the flight, the systematic delay of the 60-90 keV channel with respect to 90-150 keV electrons amounted to 0.01 ± 0.01 sec. A secondary cross-correlation maximum near 1.2 seconds is evident. This feature arises from the roughly periodic 1.2 second recurrence pattern of the larger microbursts seen during this flight.

Finally we note that, although intense precipitation was observed at 7 and 13 keV, it showed no evidence whatsoever of short-term time structure. During order-of-magnitude flux variations above 60 keV, the channeltron count rates varied by less than 10%. However, assuming an exponential energy

dependence and extrapolating the scintillation counter energy spectrum back to 7 and 13 keV, we expect a contribution here of only 1% to 3% arising from microburst electrons.

Three seconds of weaker precipitation, characteristic of the first portion of this 17 September flight, are illustrated in Figure 6. Here again the impulsive nature of the electron fluxes is apparent; however, the strength of this precipitation is smaller by a factor of about twenty, and there is an obvious systematic delay of 60-90 keV electrons with respect to the higher channels. A cross-correlation analysis of a forty second stretch of these data reveals a significant maximum centered on 0.10 sec. delay for 60-90 keV against 90-150 keV, and centered on 0.26 sec. for 60-90 keV against 150-300 keV. Other characteristics of these microbursts are the roughly 1.2 sec. spacing of the maxima, the 0.2 sec. characteristic width of the impulses, and an e-folding energy of approximately 15 keV. They are similar in most respects, then, to microbursts seen in the episode described above.

DISCUSSION

Although it is possible to construct electron source models containing any degree of inherent dispersion, the data presented here permit a simpler interpretation based on the dependence of travel time upon electron energy. First, the prompt appearance of intense-microburst electrons over a large range of energies indicates that the immediate source of electrons must lie nearby ($2 \pm 2\ R_e$) and must be synchronous, i.e. affect the precipitation of all electron energies at the same time. Second, given that the source acts synchronously, the distance required to explain the large systematic delay of lower energy weak-microburst electrons seen early in the flight is $22 \pm 6\ R_e$.

This larger distance is suggestive of the length of a closed magnetic field line connecting northern and southern hemispheres near the noon meridian. The actual local time of the launch was 10:44, and the relevant geomagnetic latitude is 69°. A dipole field line at this latitude would have a length of 24 R_e, while the compressed magnetic model of Mead (1964) indicates a length of approximately 19 R_e. Consequently, the assumption that the mechanism responsible for microbursts acts synchronously will require that it be operable at each end of the closed field line. Because both Ft. Churchill and its conjugate point were sunlit and passing through mid-morning hours during this flight, and because those two conditions are apparently necessary for the appearance of microburst activity, we cannot rule out the possibility of southern hemisphere activity, and indeed might very well expect to see it under these conditions.

SUMMARY

1. Impulsive energetic electron precipitation, accompanied by steady low energy electron fluxes, has been observed from a sounding rocket.
2. The observed time structure and energy spectra permit identification of these impulses as responsible for X-ray microbursts.
3. Time-of-travel arguments suggest that, although the source of their energy is known, the impulsive dumping of the energetic electrons is organized within approximately 4 R_e of the surface of the earth, and can occur in either hemisphere.

Acknowledgments. I am indebted to Professor Kinsey Anderson for his helpful guidance throughout this study.

The rocket flights reported herein were supported by the National Aeronautics and Space Administration, [redacted] through

grant NsG-337. The associated balloon flights were funded by the National Science Foundation through grant GP2252, with logistic support provided by the Office of Naval Research.

REFERENCES

Anderson, K. A., and D. W. Milton, Balloon observations of X-rays in the auroral zone; Part 3, High time resolution studies, J. Geophys. Res. 69, 4457-4479, 1964.

Anderson, K. A., L. M. Chase, H. S. Hudson, M. Lampton, D. W. Milton, and G. K. Parks, Balloon and rocket observations of auroral zone microbursts, J. Geophys. Res. 71, 4617-4630, 1966.

Barcus, J. R., and A. Christensen, A 75-second periodicity in auroral zone X-rays, J. Geophys. Res. 70, 5455-5459, 1965.

Barcus, J. R., and T. J. Rosenberg, Observations on the spatial structure of pulsating electron precipitation accompanying low frequency hydromagnetic disturbances in the auroral zone, J. Geophys. Res. 70, 1707-1716, 1965.

Barcus, J. R., and T. J. Rosenberg, Energy spectrum for auroral zone X-rays, J. Geophys. Res. 71, 803-823, 1966.

Blake, J. B., S. C. Freden, and G. A. Paulikas, Precipitation of 400-keV electrons in the auroral zone, J. Geophys. Res. 71, 5129-5134, 1966.

Brown, R. R., Electron precipitation in the auroral zone, Space Science Reviews 5, 311-387, 1966.

Chamberlain, J. W., Plasma instability as a mechanism for auroral bombardment, J. Geophys. Res. 68, 5667-5676, 1963.

Coppi, B., Role of plasma instabilities in auroral phenomena, Nature 205, 998, 1965.

Hudson, H. S., G. K. Parks, D. W. Milton, and K. A. Anderson, Determinations of the auroral zone X-ray spectrum, J. Geophys. Res. 70 4979-4982, 1965.

McDiarmid, I. B., and E. E. Budzinski, Angular distributions and energy spectra of electrons associated with auroral events, Can. J. Phys. 42, 2048, 1964.

Mead, G. D., Deformation of the geomagnetic field by the solar wind, J. Geophys. Res. 69, 1181-1195, 1964.

Mozer, F. S., Rocket measurements of energetic particles; 2, Electron results, J. Geophys. Res. 70, 5709-5716, 1965.

O'Brien, B. J., High latitude geophysical studies with satellite Injun 3; Part 3, Precipitation of electrons into the atmosphere, J. Geophys. Res. 69, 13-43, 1964.

FIGURE CAPTIONS

Figure 1. Differential electron intensities and vehicle aspect angle as functions of time and altitude. Two second averages have been taken.

Figure 2. Representative energy spectra for pitch angles 5-35°.

Figure 3. Polar plots of four pitch angle distribution obtained from the 60-90 keV energy channels.

Figure 4. Three seconds of impulsive electron precipitation seen in several energy channels. Effects of rocket spin have not been removed here from the radial scintillator record.

Figure 5. Cross correlation function for the more intense microbursts. Points are plotted at intervals of 0.01 sec.

Figure 6. Three seconds of weaker impulsive electron precipitation, obtained earlier in the flight. Spin modulation has not been removed here.

Figure 7. Cross correlation function for 40 sec of data including that of Figure 6.

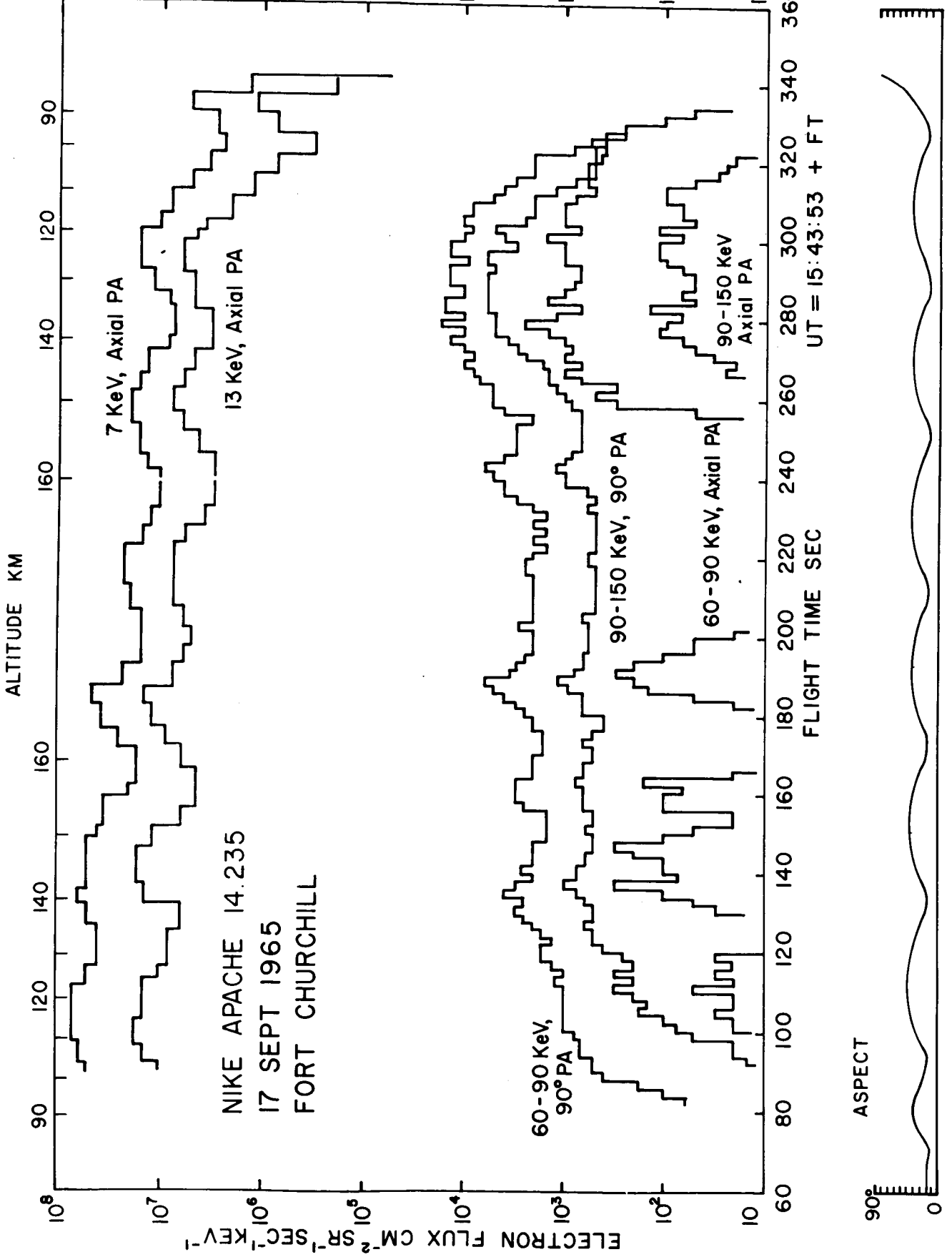
ELECTRON FLUX CM⁻²SR⁻¹SEC⁻¹KEV⁻¹
ALTITUDE KM
FLIGHT TIME SEC
UT = 15:43:53 + FT
NIKE APACHE 14.235
17 SEPT 1965
FORT CHURCHILL
7 KeV, Axial PA
13 KeV, Axial PA
60-90 KeV, 90° PA
90-150 KeV, 90° PA
60-90 KeV, Axial PA
90-150 KeV Axial PA
ASPECT
90°
0

Figure 1.

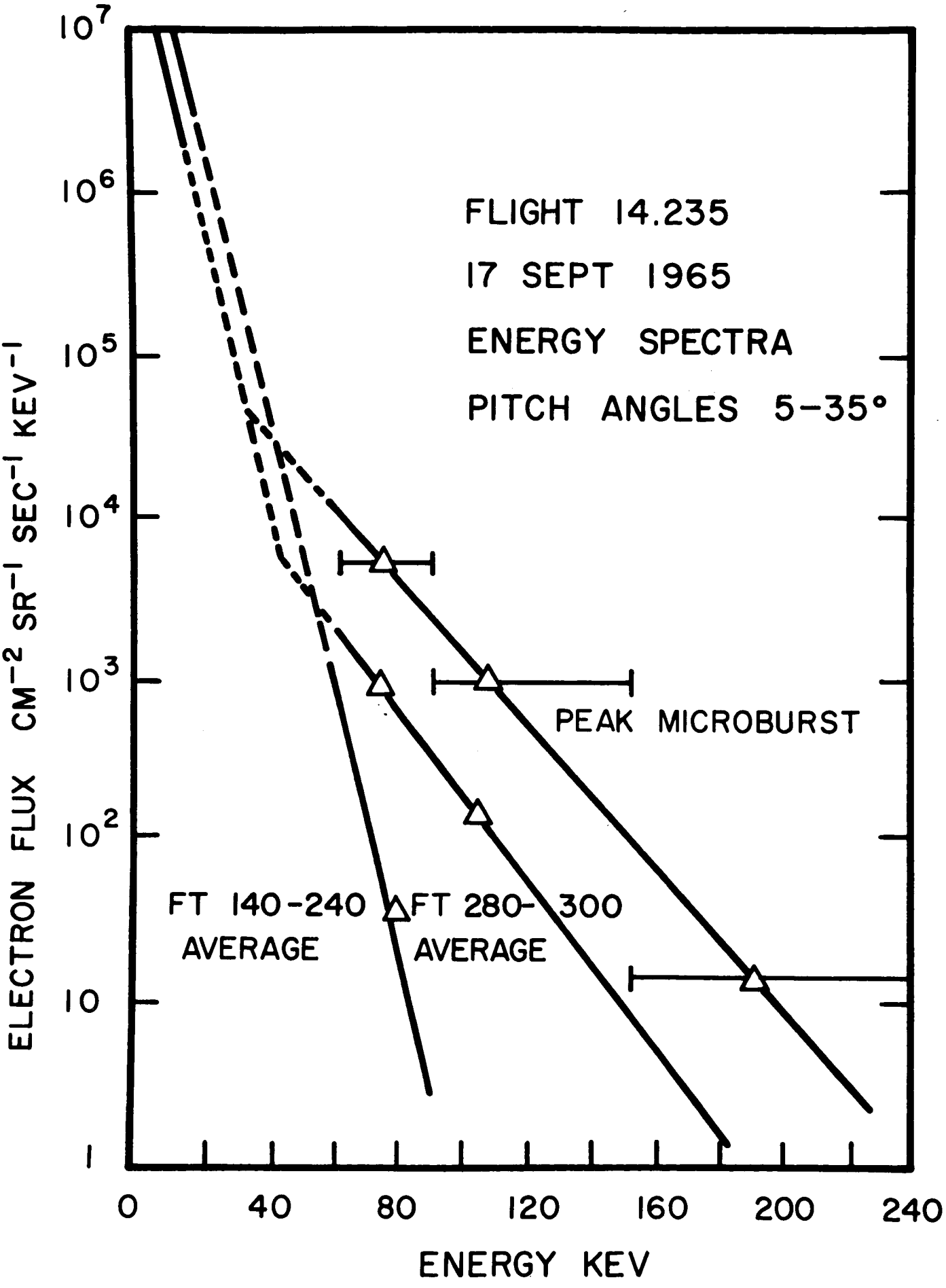
FLIGHT 14.235
17 SEPT 1965
ENERGY SPECTRA
PITCH ANGLES 5-35°
PEAK MICROBURST
FT 140-240 AVERAGE
FT 280-300 AVERAGE
ELECTRON FLUX CM⁻² SR⁻¹ SEC⁻¹ KEV⁻¹
ENERGY KEV
10⁷
10⁶
10⁵
10⁴
10³
10²
10
1
0
40
80
120
160
200
240

Figure 2.

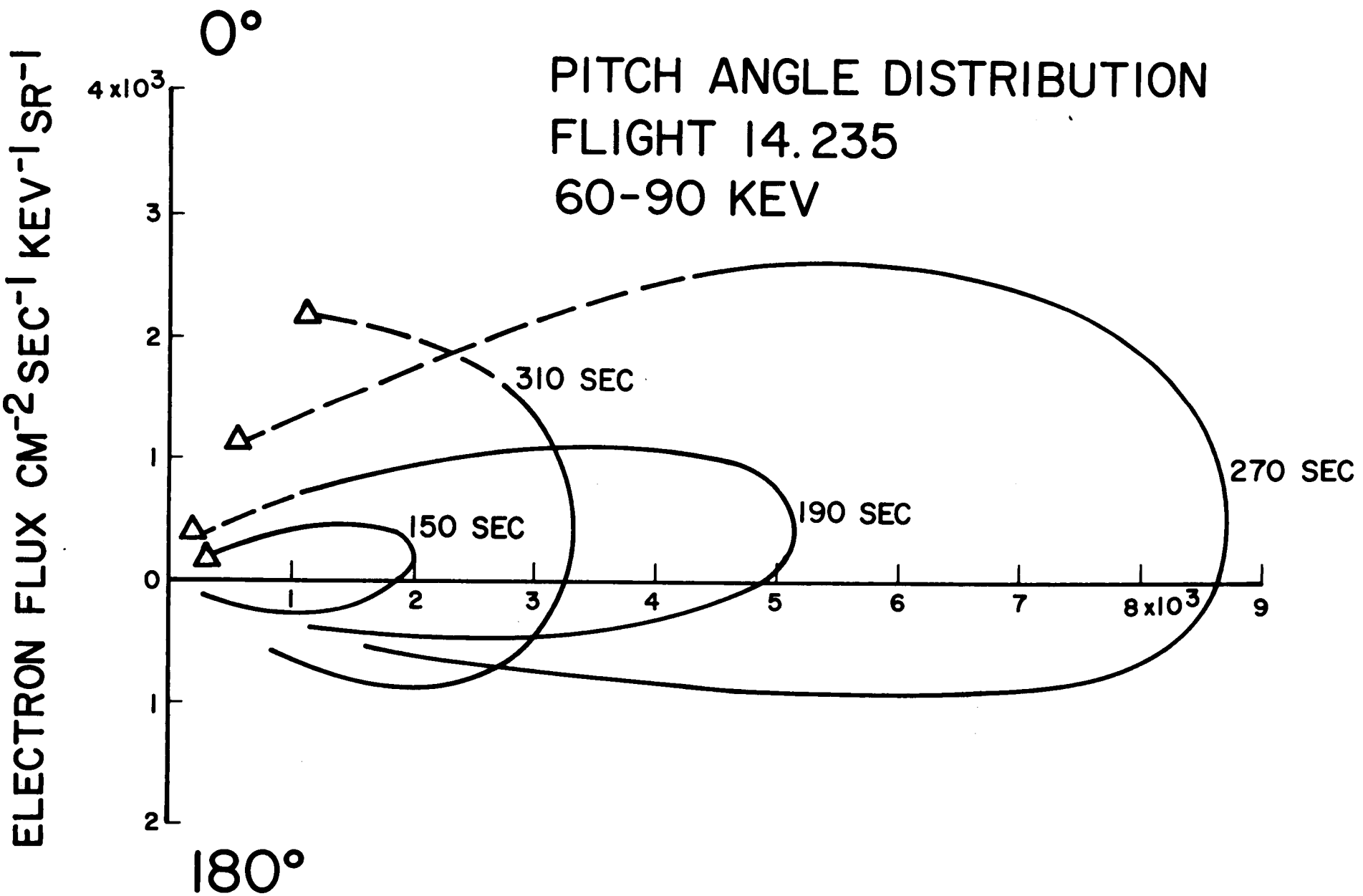
0°
PITCH ANGLE DISTRIBUTION
FLIGHT 14.235
60-90 KEV
ELECTRON FLUX CM-2 SEC-1 KEV-1 SR-1
4x10^3
3
2
1
0
1
2
310 SEC
270 SEC
190 SEC
150 SEC
1
2
3
4
5
6
7
8x10^3
9
180°

Figure 3.

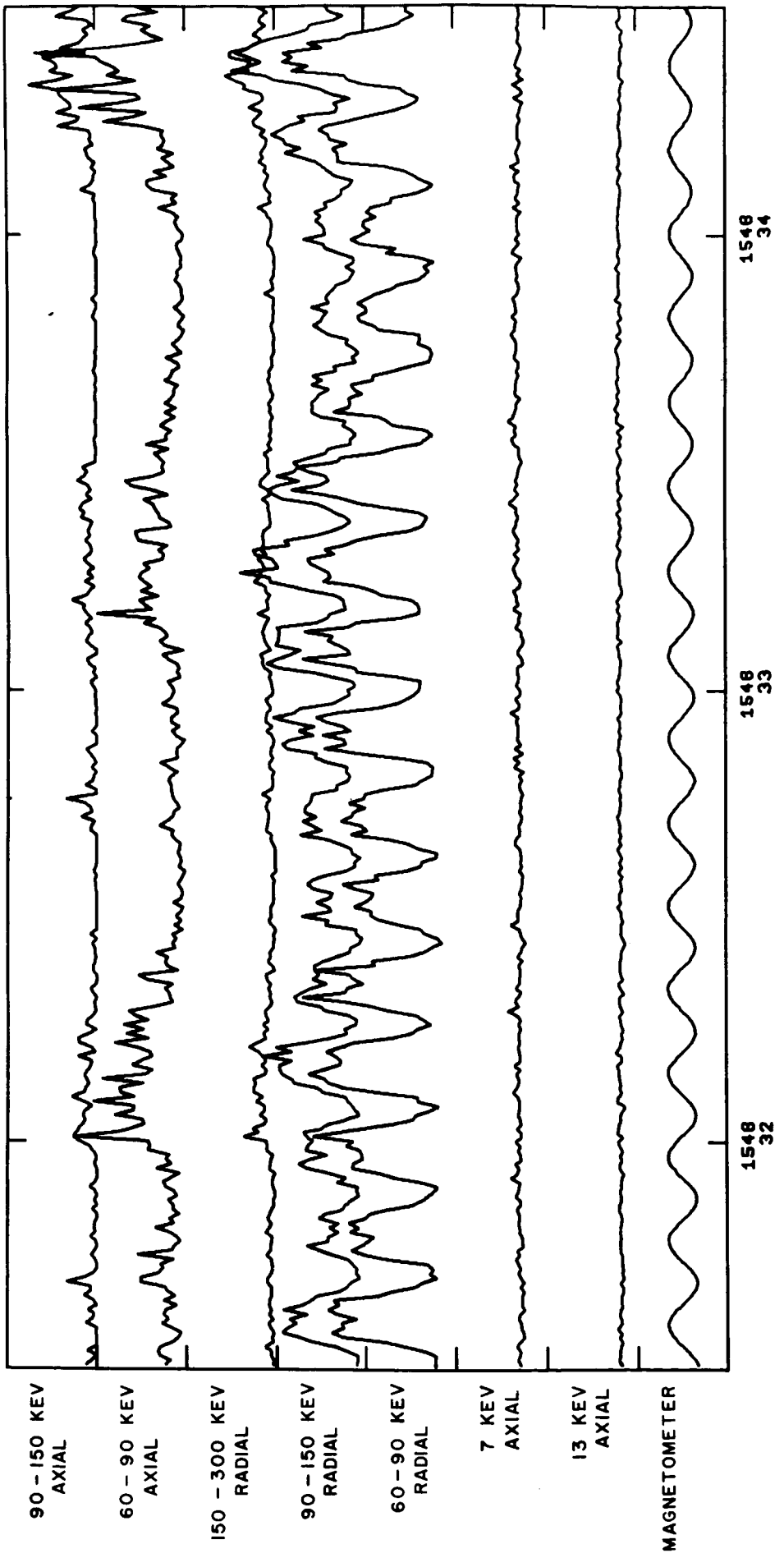
90 - 150 KEV AXIAL
60 - 90 KEV AXIAL
150 - 300 KEV RADIAL
90 - 150 KEV RADIAL
60 - 90 KEV RADIAL
7 KEV AXIAL
13 KEV AXIAL
MAGNETOMETER
1548 32
1548 33
1548 34

Figure 4.

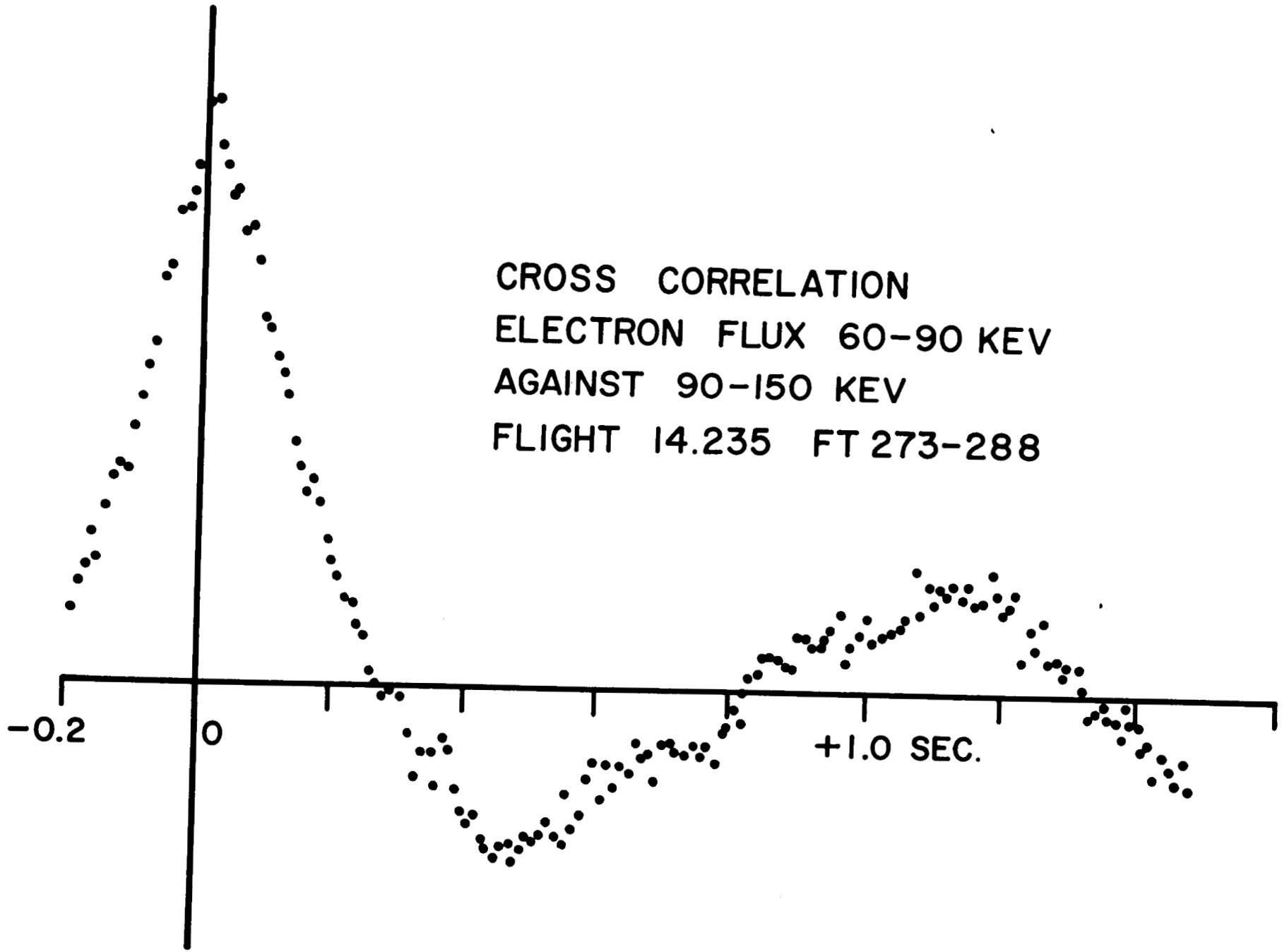
CROSS CORRELATION
ELECTRON FLUX 60-90 KEV
AGAINST 90-150 KEV
FLIGHT 14.235 FT 273-288
-0.2
0
+1.0 SEC.

Figure 5.

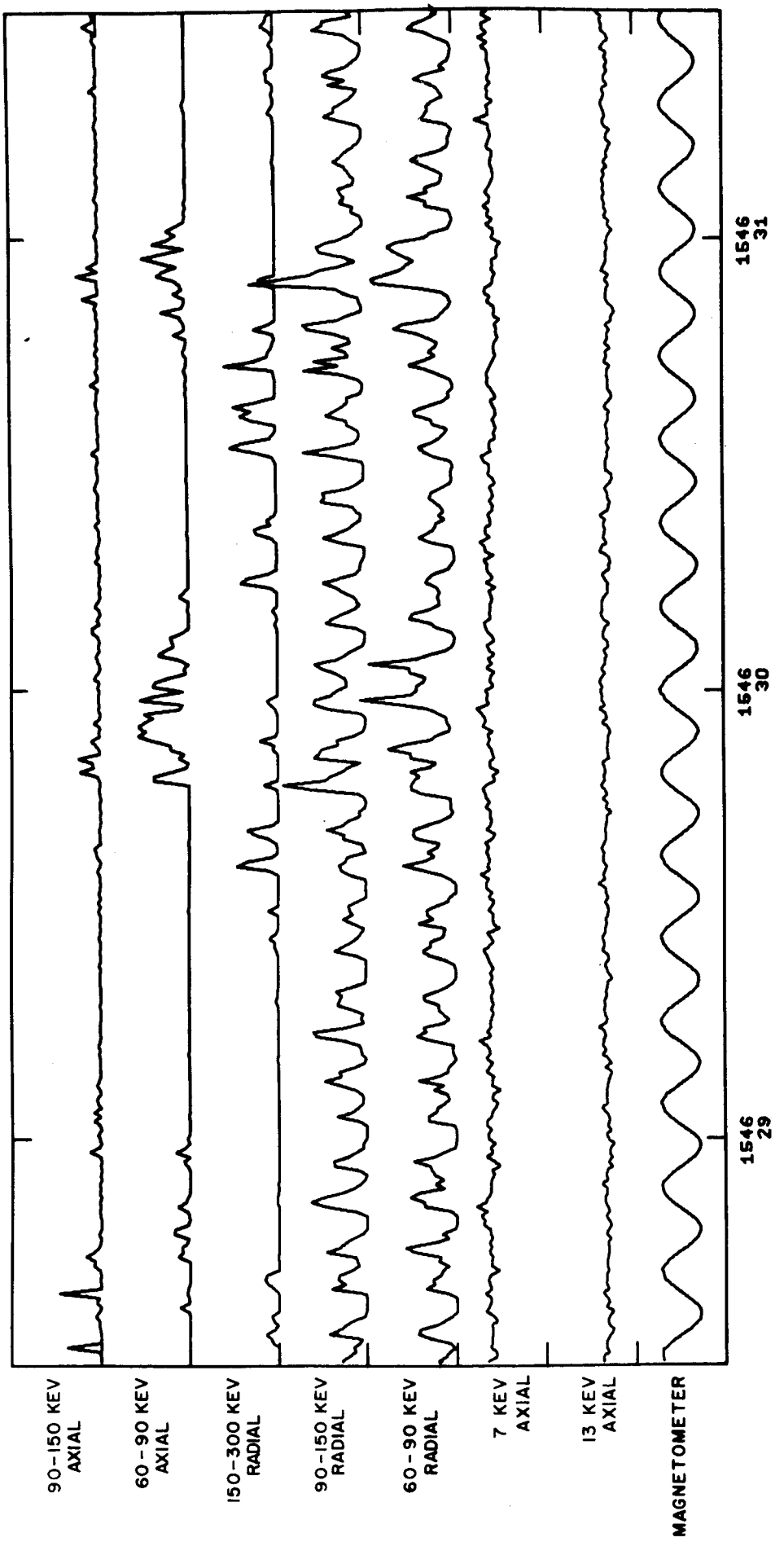
90-150 KEV AXIAL
60-90 KEV AXIAL
150-300 KEV RADIAL
90-150 KEV RADIAL
60-90 KEV RADIAL
7 KEV AXIAL
13 KEV AXIAL
MAGNETOMETER
1546 29
1546 30
1546 31

Figure 6.

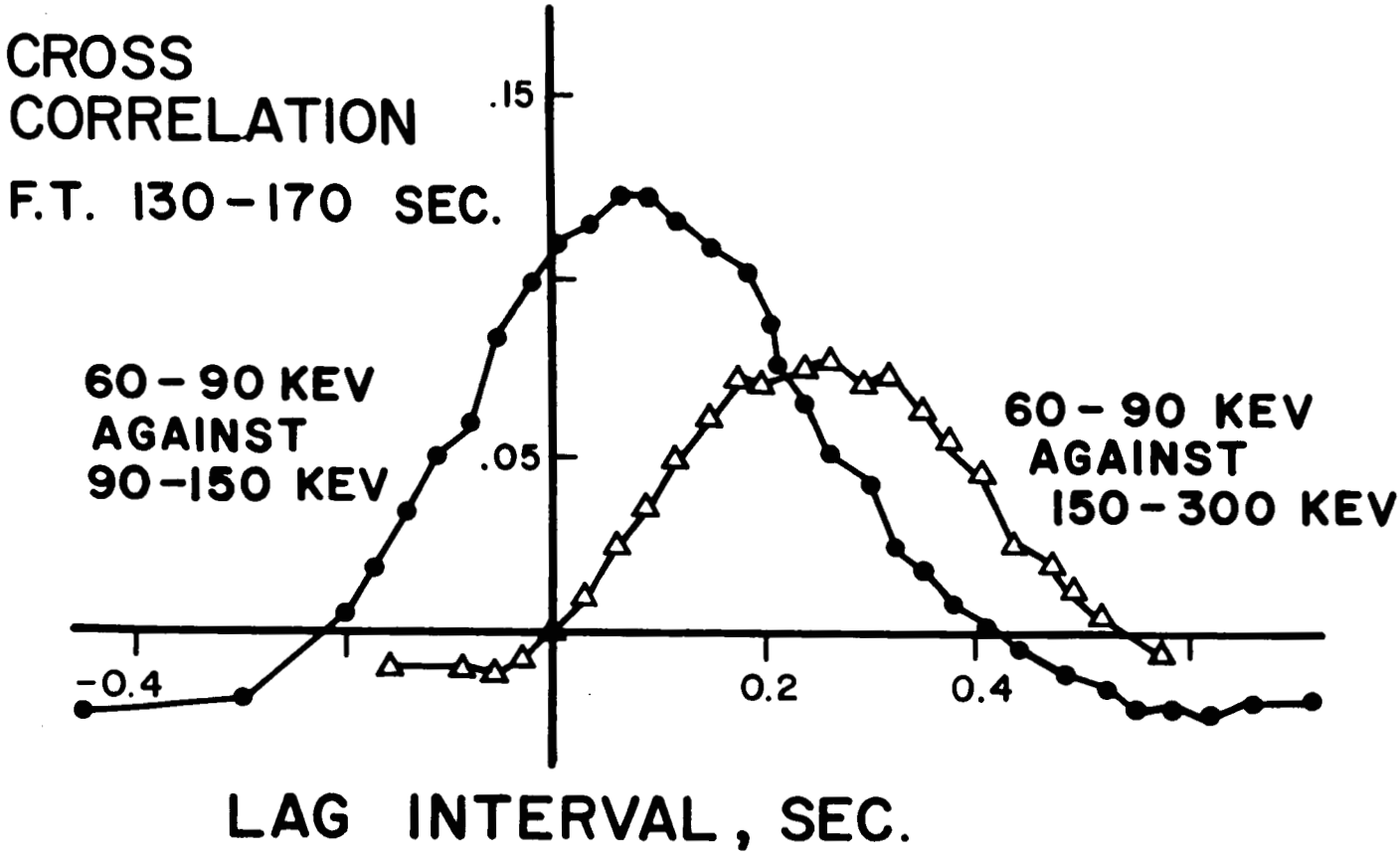
CROSS
CORRELATION
F.T. 130-170 SEC.
.15
.05
60-90 KEV
AGAINST
90-150 KEV
60-90 KEV
AGAINST
150-300 KEV
-0.4
0.2
0.4
LAG INTERVAL, SEC.

Figure 7.